Characterization of PKD Protein-Positive Exosome-Like Vesicles

Marie C. Hogan,* Luca Manganelli,*† John R. Woollard,* Anatoliy I. Masyuk,‡ Tatyana V. Masyuk,‡ Rachaneekorn Tammachote,* Bing Q. Huang,‡ Alexey A. Leontovich,§ Thomas G. Beito,‖ Benjamin J. Madden,¶ M. Cristine Charlesworth,¶ Vicente E. Torres,* Nicholas F. LaRusso,‡ Peter C. Harris,* and Christopher J. Ward*

*Division of Nephrology and Hypertension, ‡Center for Basic Research in Digestive Diseases, §Bioinformatics Core Facility, Division of Biomedical Informatics, ‖Mayo Ab Core, and ¶Mayo Proteomics Core, Mayo Clinic, Rochester, Minnesota; and †Department of Nephrology, University of Modena and Reggio Emilia, Modena, Italy

ABSTRACT

Proteins associated with autosomal dominant and autosomal recessive polycystic kidney disease (polycystin-1, polycystin-2, and fibrocystin) localize to various subcellular compartments, but their functional site is thought to be on primary cilia. PC1+ vesicles surround cilia in *Pkhd1*$^{del2/del2}$ mice, which led us to analyze these structures in detail. We subfractionated urinary exosome-like vesicles (ELVs) and isolated a subpopulation abundant in polycystin-1, fibrocystin (in their cleaved forms), and polycystin-2. This removed Tamm-Horsfall protein, the major contaminant, and subfractionated ELVs into at least three different populations, demarcated by the presence of aquaporin-2, polycystin-1, and podocin. Proteomic analysis of PKD ELVs identified 552 proteins (232 not yet in urinary proteomic databases), many of which have been implicated in signaling, including the molecule Smoothened. We also detected two other protein products of genes involved in cystic disease: Cystin, the product of the mouse *cpk* locus, and ADP-ribosylation factor-like 6, the product of the human Bardet-Biedl syndrome gene (*BBS3*). Our proteomic analysis confirmed that cleavage of polycystin-1 and fibrocystin occurs *in vivo*, in manners consistent with cleavage at the GPS site in polycystin-1 and the proprotein convertase site in fibrocystin. *In vitro*, these PKD ELVs preferentially interacted with primary cilia of kidney and biliary epithelial cells in a rapid and highly specific manner. These data suggest that PKD proteins are shed in membrane particles in the urine, and these particles interact with primary cilia.

J Am Soc Nephrol 20: 278–288, 2009. doi: 10.1681/ASN.2008060564

Autosomal dominant polycystic kidney disease (ADPKD) is the most common hereditary renal disease, affecting between 1:400 to 1:1000 individuals.[1,2] There are two genetic loci, *PKD1* and *PKD2*, producing the proteins polycystin-1 (PC1)[3–5] and polycystin-2 (PC2),[6] respectively. Autosomal recessive polycystic kidney disease (ARPKD), the most common cause of hereditary childhood PKD, is caused by mutations to *PKHD1*, which encodes fibrocystin/polyductin (FCP).[7,8] These three PKD proteins have been localized to primary cilia,[9,10] where the PC1/PC2 complex acts as a flow sensor on the cilium.[11] The role of FCP is less clear, but it complexes with PC2.[12,13]

Another site of PC1 expression is in urinary exosomes, small vesicles (50 to 100 nm in diameter) present in normal urine, that have been analyzed as a source of biomarkers for various renal diseases.[14,15] Urinary exosomes are thought to be end products

Received June 2, 2008. Accepted September 5, 2008.

Published online ahead of print. Publication date available at www.jasn.org.

Correspondence: Dr. Christopher J. Ward, Division of Nephrology & Hypertension, Mayo Clinic, 200 First Street SW, Rochester, MN 55905. Phone: 507-266-3050; Fax: 507-266-9315; E-mail: ward.christopher@mayo.edu

of the multivesicular body (MVB)-sorting pathway in which membrane proteins are uniquely packaged into intraluminal vesicles (ILVs) within the MVB, some of which are secreted as exosomes when MVBs fuse with the apical plasma membrane.

MVBs and exosomes have been shown to have a role in left/right (L/R) axis determination in the embryonic node. These MVBs, termed nodal vesicular parcels (NVPs), are released from the floor of the node and swept by nodal flow to the left side, where they interact with the "picket-fence" immotile cilia.[16] Symmetry breaking is dependent on a PC2 Ca^{2+}-dependent flux.[17,18]

Transmission electron microscopy studies of dilated bile ducts found in ARPKD mouse model *Pkhd1*$^{del2/del2}$ showed PC1+ exosome-like vesicles surrounding cholangiocyte primary cilia, whereas only occasional single ELVs were found attached to WT cilia.[19] The observations of abundant PC1 in ELVs and of abnormal ELV accumulation in FCP-deficient mice led us to examine whether these may have a functional role in the urinary and biliary systems, analogous to the NVP in the node.

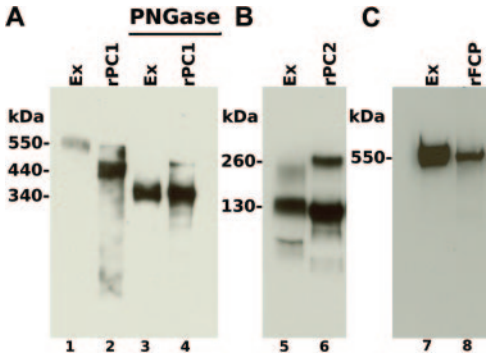

Figure 1. Western analysis shows urinary ELVs are enriched for PC1, PC2, and FCP. (A) Comparison of ELV (Ex) (lane 1) and exogenously expressed PC1 (rPC1; 5 μg membrane protein (lane 2) and after PNGase treatment (lanes 3 and 4), detected with PC1 mAb (7e12). ELV PC1 seems to be heavily glycosylated and similar in size to unGPS cleaved PC1 (550 kD), but after deglycosylation is similar in size (340 kD) to the GPS cleaved rPC1. (B) Detection of PC2 in ELVs (Ex; lane 5) and rPC2 (lane 6) with the PC2 antisera YCC2 shows a 130-kD product in both—a probable dimer is also seen with exogenously expressed PC2 (lane 6). (C) A similar sized product (550 kD) is detected in ELVs (lane 7) and rFCP (lane 8) with the FCP mAb11.

RESULTS

To determine which PKD proteins are present in urinary ELVs and their relative size with respect to recombinant protein, we prepared a crude preparation. Western analysis compared this ELV preparation with exogenously expressed full-length proteins in PEAK cells (human embryo kidney cells) using antibodies to the LRR region of PC1 (7e12),[20] the N-terminus of FCP and to the C-terminus of PC2.[21] Strong signals were detected using just 2 μg of total ELV protein (compared with 10 to 50 μg of kidney membrane preparation used in previous studies of renal cells to detect PC1[20]), with the product sizes consistent with the predicted and recombinant glycosylated molecular weight of two of the proteins: PC2, 130 kD; and FCP, 500 to 550 kD (Figure 1, B and C). However, the PC1 in ELVs was appreciably larger than the recombinant PC1 (Figure 1A). To confirm that PC1 was specifically detected, we deglycosylated both ELV and recombinant PC1. In this case, both the recombinant and ELV PC1 co-migrated at approximately 340 kD (predicted 325 kD), confirming identity and showing that ELV PC1 has extensive N-linked glycosylation.

Purification of PKD-ELVs

To obtain significant quantities of urinary ELVs, we developed a scaled-up modification of the procedures of Pisitkun *et al.*[14] and Zhou *et al.*[15] The material generated by this protocol is rich in the most abundant urinary protein, Tamm-Horsfall protein (THP; also known as uromodulin). Electron microscopic studies showed that THP formed long higher order fibrils that were contaminating the exosomal preparations (Figure 2D). Initially, we attempted to remove the THP using sucrose gradients in normal water, but the THP and PKD-ELVs co-banded. We therefore increased the density of the gradient using heavy water. The crude ELVs were fractionated by density ultracentrifugation on a D_2O 5 to 30% sucrose gradient (Figure 2, A through D). Western analysis of fractions from these gradients showed that the bulk of the THP pelleted and that fractions 8 and 9 were enriched for PC1. The peak refractive index for the PKD-ELVs was $\eta = 1.3530$ (SD $\pm$ 0.0019; $n = 6$), representing a density of approximately 1.17 kg/L in D_2O. By using this gradient, we were able to remove >99% of the THP from the ELVs and to isolate 100 μg of PC1-enriched ELVs per liter of urine, <1% of the initial protein in the crude ELV preparation (Figure 3, A and B). The stem cell marker CD133 (prominin) also co-sediments with PC1, PC2, and FCP. This contrasted with other proteins previously detected in urinary ELVs that were found in different fractions: Aquaporin 2, in fractions 1 through 5, and the steroid-resistant nephrotic syndrome protein, podocin (NPHS2), that was enriched in fractions 10 through 14 (Supplemental Figure 1).

The morphology of the PKD-ELVs was similar to a "deflated football" with concave and convex sides. Diameters ranged from 66.1 to 187.0 nm, with a mean of 107 nm (SD $\pm$22.1; $n = 56$; Figure 2, E through I), overlapping in range with the measurements reported by Pisitkun *et al.*[14] Immunoelectron microscopic analysis of the PKD-ELVs showed that PC1, FCP, and CD133 all co-localize with PC2.

Proteomic Analysis of the PKD-ELVs

To characterize the full range of proteins in the PKD-ELVs, we undertook a proteomic analysis of this fraction. Because many ELV proteins are extensively glycosylated, we analyzed ELVs with and without peptide:N-glycosidase F treatment to remove N-linked sugars. ELVs were prepared from four healthy adults (two male and two female), and the PC1+ peak fractions were

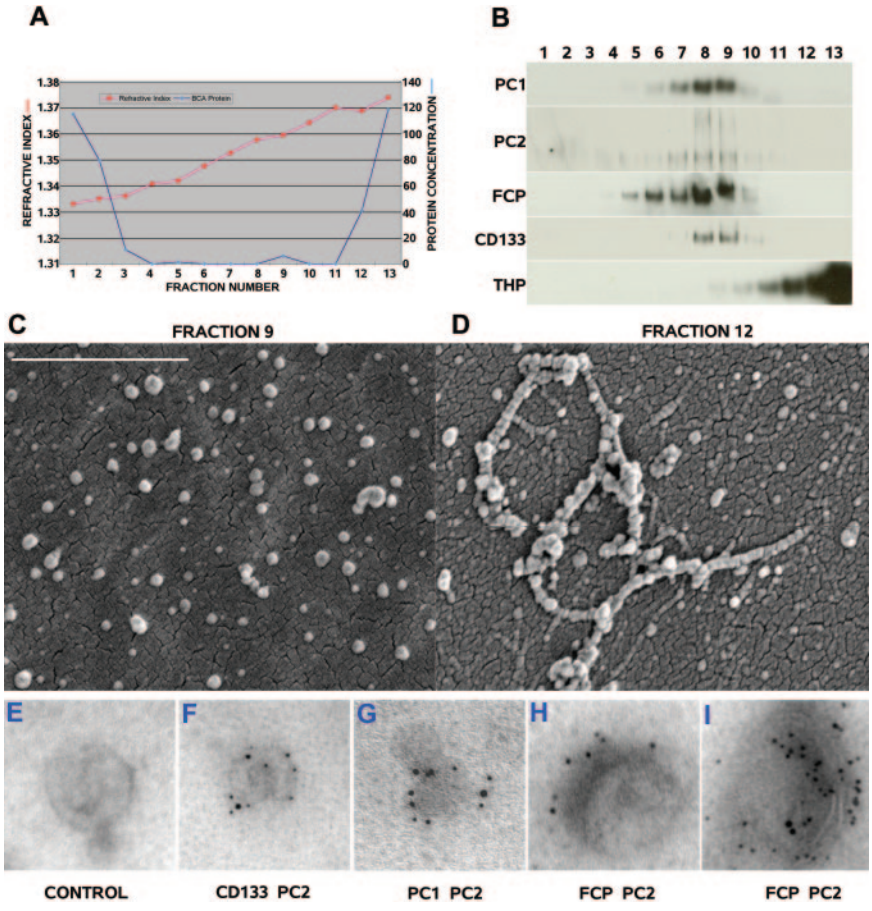

Figure 2. Purification of human urinary ELVs on a 5 to 30% sucrose gradient in D_2O. (A) Refractive index profile (in red) ranging linearly from $\eta = 1.33$ to 1.37 and protein concentration of the fractions (in blue) in μg/ml. Most of the protein is in the first three and last two fractions. (B) Distribution of PC1, PC2, FCP, and CD133, which co-band in fractions 7, 8, and 9. THP is present in the pellet and the last three fractions. (C) SEM of PKD-ELVs bound to poly-L-lysine coverslips from fraction 9 (bar = 1 μm) and (D) ELVs and fibrils of THP from fraction 12 (same scale as in C). (E through I) ImmunoEM shows that PC1, PC2, FCP, and CD133 are co-localized on ELVs. (E) Control (no primary antibody) on negatively stained ELVs. (F) PC2 (10 nm gold) and CD133 (5 nm gold), (G) PC2 (10 nm gold) and PC1 (5 nm gold), (H) PC2 (10 nm gold) and FCP (5 nm gold), and (I) a large multilaminate ELV, PC2 (10 nm gold), and FCP (5 nm gold) suggesting a MVB origin for PKD-ELVs.

pooled. These were then run on a 4 to 12% PAGE gel that was sectioned into 35 separate slices (Figure 3, B and C). To enrich for genuine PKD-ELV proteins, we analyzed in detail only those with at least three unique peptides and 10% coverage in both glycosylated and unglycosylated samples, a total of 552 proteins (Supplemental Database 1).

Presence of PC1, PC2, and FCP and Interacting Partners

Pisitkun *et al.*[14] showed that PC1 was present in a relatively crude preparation of urinary exosomes by both proteomics and Western blotting. We focused on a subfraction of ELVs in the urine and were able to show that PC2 and FCP are also present, because the PKD-ELVs are more concentrated, permitting detailed analysis of their contents by mass spectrometry. Ranking proteins by the total number of unique peptides (in the deglycosylated data set), FCP (PKHD1_HUMAN; 80 peptides, coverage 30%) is one of the most highly represented, ranked second; PC1 (PKD1_HUMAN; 42 peptides, coverage 13%), also ranked highly at 15th, and PC2 (PKD2_HUMAN; 21 peptides, coverage 25%) ranked 90th. This reinforces that they are abundant in ELVs; however, when this proteome is ranked as a function of the percentage protein coverage by peptides, FCP is 376th, PC2 is 416th, and PC1 is 528th (Table 1).

We surveyed the literature for described PC1-, PC2-, and FCP-interacting proteins defined by yeast two-hybrid and other analysis and ranked these by percentage coverage by unique peptides (Table 1). The PC2-interacting proteins CD2AP (CD2AP_HUMAN; rank 126, 39 peptides, 60% coverage)[22] and α-actinin-1 (ACTN1_HUMAN; rank 511, five peptides, 15% coverage)[23] were present. The Na/K-transporting ATPase α-1 chain precursor (EC 3.6.3.9; AT1A1_HUMAN; rank 226, 46 peptides, 46% coverage), a described PC1-interacting protein, was also present.[24] $G_{(i)}\alpha 1$ subunit (GNAI1_HUMAN; rank 54, 11 peptides, 71% coverage), $G_{(i)}\alpha 2$ subunit (GNAI2_HUMAN; rank 81, 19 peptides, 67% coverage), and $G_{(q)}\alpha$ subunit (GNAQ_HUMAN; rank 187, 8 peptides, 52% coverage) were also observed (Table 1). These α subunits have been shown to interact with 74 amino acids (aa) in the cytoplasmic C-terminal tail of mouse PC1.[25,26]

In Vivo Cleavage of PC1 and FCP Assessed by Peptide Distribution

Both FCP and PC1 are thought to be cleaved within their extracellular domains,[27–29] but many of these data were derived from overexpressing full-length cDNAs in cell lines. Proteomic analysis of the PKD-ELVs allowed assessment of cleavage of the *in vivo* products without the need for antibodies to different regions of the proteins. Cleavage data for PC1 and FCP were derived from the distribution of peptides on the gel in the glycosylated run (the deglycosylated run had some smearing probably as a result of incomplete deglycosylation; Figure 3). A total of 32 peptides to

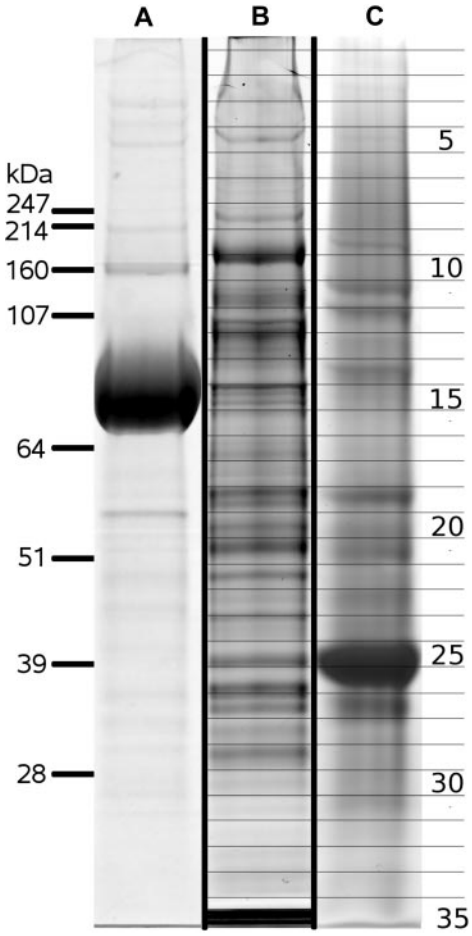

Figure 3. Coomassie stained 4 to 12% SDS-PAGE gels of urinary ELVs. (A) A total of 30 μg of crude ELVs prepared by ultracentrifuging urine at 150,000 $\times$ *g* for 1 h. Note the large amount of THP centered at approximately 85 kD. (B) A total of 30 μg of pure PKD-ELVs; note the lack of a prominent THP band. (C) A total of 30 μg of pure PKD-ELVs that have been deglycosylated with PNGase F; note the prominent PNGase F band at 36 kD. The 35 gel slices selected for the proteomic analysis are shown.

PC1 were in gel slice 4 (approximately 500 kD); these peptides all were N-terminal to the G protein–coupled receptor proteolytic site (GPS) site at aa3048; the most C-terminal peptide ended at aa2865 (Figure 4A, Supplemental Figure 2). There was one peptide in gel slice 8 and four in gel slice 10 (approximately 150 kD; Figure 3B), all of which mapped C-terminal to the GPS site, the most N-terminal peptide started at aa3190 (Figure 4A, Supplemental Figure 3). Hence, these data are consistent with a GPS cleavage event at 3048..3049,[28,29] an N-terminal fragment of approximately 500 kD and a C-terminal fragment of approximately 150 kD with a cleavage point occurring between aa2865 and aa3190. No other slices contained PC1 peptides.

In FCP, we identified 41 peptides in the glycosylated run. In slices 3 and 4 (approximately 500 to 550 kD), there were 39 peptides, the farthest C-terminal ending at aa3609. In gel slice 18 (approximately 55 to 60 kD), there were two peptides, the most N-terminal ending starting at aa3661 (Figure 4B, Supplemental Figure 3). This supports the work of Kaimori *et al.*,[27] who postulated a cleavage event at the proprotein convertase site (RAKRKR 3615..3620). The unglycosylated mass of this C-terminal fragment was 49.8 kD, and there are three potential N-linked glycosylation sites in the extracellular region of the fragment. This is powerful independent evidence of extracellular cleavage of these two proteins.

Presence of Proteins Derived from Genes Involved in Cystic Disease

More than 25 proteins causing Bardet-Biedl syndrome, nephronophthisis, Meckel-Gruber syndrome, Senior-Løken syndrome, Joubert syndrome, and orofaciodigital syndrome and animal models of syndromic PKD have been associated with the cilium and basal body. Interestingly, only two of these proteins are observed in PKD-ELVs, the protein cystin (CYS1_HUMAN; rank 160, four peptides, 56% coverage), which is the product of the *cpk* locus in mice,[10,30] and the product of the Bardet-Biedl syndrome 3 locus, ADP-ribosylation factor-like protein 6 (ARL6_HUMAN; rank 341, five peptides, 33% coverage).[31,32]

Comparison with Other Urinary Proteomes

We compared the PKD-ELV proteome with two others: The Pisitkun proteome of crude ELVs and the Adachi proteome of entire urine.[33] The data showed that PKD-ELVs had 232 unique proteins not found in the Adachi or Pisitkun sets; 191 proteins were shared between the Pisitkun and PKD-ELVs data set, and 245 were shared with the total urine proteome of Adachi; 116 proteins were shared among all three sets. This clearly shows that the PKD-ELVs represent a novel protein set (Figure 4C, Supplemental Database 1b).

In Vivo Interaction of PKD-ELVs and Primary Cilia in Human and Mouse ARPKD

Transmission electron microscopy analysis of kidney from a patient with severe ARPKD (T36M, V1627F) showed that the primary cilia were surrounded by small vesicles, some of which were closely applied to the shaft of the cilium (Figure 5, A and B). Observations made in the *Pkhd1*$^{del2/del2}$ mouse indicated that primary cilia in the mouse biliary tree were also associated with small vesicles, some of which were attached to the cilium (Figure 5D).[19] To quantify this phenomenon, we counted the number of adherent ELVs per micrometer on wild-type (WT) and *Pkhd1*$^{del2/del2}$ biliary cilia. In WT mice (Figure 5C), we found 1.45 ELVs/μm (SD $\pm$1.32; $n = 5$ cilia; 6.5 μm total length), and in *Pkhd1*$^{del2/del2}$ biliary cilia, we found 31.1 ELVs/μm (SD $\pm$5.9; $n = 4$ cilia; 5.45 μm total length; $P < 0.02$, two-sample test, normal approximation). Staining *Pkhd1*$^{del2/del2}$ biliary epithelia with our anti-PC1 mAb, 7e12, showed that these primary cilium-interacting vesicles were PC1+ (Figure 6, A and B) and that similar structures were present in MVBs as ILVs in normal rat biliary epithelium (Figure 6, F and G). PC1 was localized to the primary cilium in several studies.[10,11,34] We show that the apical membrane and much of the shaft of the WT primary cilium

Table 1. PC1-interacting proteins found in PKD-ELVs[a]

Names	Rank (UP)	Unique Peptides	Rank (C)	% Coverage
Polycystic kidney and hepatic disease 1 precursor (fibrocystin)	2	80	376	30
ADPKD protein 1 (PC1)	15	42	528	13
PC2 (PKD 2 protein)	93	21	416	25
CD2-associated protein	22	39	126	60
Na^+/K^+-transporting ATPase α-1 chain precursor	14	46	226	45
α-Actinin-1	444	5	511	15
Guanine nucleotide-binding protein $G_{(i)}$, α-1 subunit	231	11	54	71
Guanine nucleotide-binding protein $G_{(i)}$, α-2 subunit	112	19	81	67
Guanine nucleotide-binding protein $G_{(q)}$ subunit a	328	8	187	52

[a]Rank (UP) refers to rank by number of unique peptides found in the proteome of the PNGase-treated run. Rank (C) refers to the rank derived from the percentage of the protein covered by unique peptides in the PNGase-treated run.

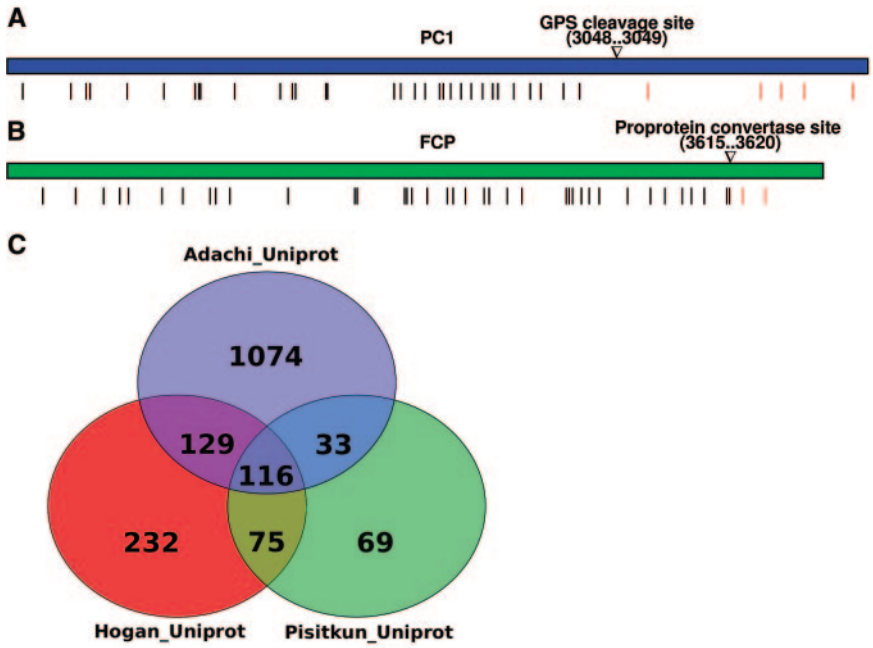

Figure 4. Cleavage of PC1 and FCP and comparison of PKD-ELV proteome with other urinary proteomes. (A) The PC1 protein with the GPS cleavage site at aa 3048..3049. Peptides found in gel slice 4 (approximately 500 to 550 kD) are represented by black bars; peptides found in gel slices 8 and 10 (approximately 150 kD) are represented by red bars (Supplemental Figure 2). (B) The FCP protein with the proprotein convertase consensus at 3615..3620. Peptides found in gel slices 3 to 4 (approximately 550 kD) are represented by black bars, whereas the two peptides seen in gel slice 18 (approximately 55 to 60 kD) are represented by red bars (Supplemental Figure 3). No other gel slices yielded peptides from PC1 and FCP in the glycosylated run. (C) Comparison Venn diagram of peptides found in a total urine proteome (Adachi),[14] crude urinary ELVs (Pisitkun),[33] with PKD-ELVs (our data, Hogan). Numbers represent the number of shared proteins in the respective overlapping circles. The individual sets of proteins are available in Supplemental Database 2.

is negative for PC1 but is surrounded by intensely PC1+ ELVs (PKD-ELVs; Figure 6, C and D). We also show electron microscopic micrographs showing PKD-ELVs that seem to be adhering to cilia (Figures 5; 6, A and B; 7; and 8). This may account for the PC1 staining seen on cilia by light immunofluorescence microscopy, which can be punctate in nature. We also observed a PKD-ELV emerging from an intracellular vesicle near the base of the cilium (Figure 6E). These results suggest that ELVs interact with primary cilia *in vivo* and that in *Pkhd1* mutants, ELVs accumulate on the primary cilium. Furthermore, we observed a 1- to 2-μm MVB interacting with a primary cilium in a patient with ARPKD (Figure 5B). This event may be analogous to the *smash* event observed in the embryonic node by Tanaka *et al.*[16] Importantly, in all cases, there seemed to be two bilipid membranes at the site of attachment, suggesting an adhesive rather than a budding event (Figure 5).

In Vitro Analysis of ELV–Cilium Interactions

To test the interaction between ELVs and cilia, we surface-biotinylated urinary ELVs and purified them on a D_2O sucrose gradient. We used polarized inner medullary collecting duct (IMCD3) cells and sections of WT rat biliary tree biliary units (BUs) as targets for interaction. Target cells were incubated for 1, 2, 5, and 10 min with biotinylated ELVs. The interaction was then stopped using 2.5% glutaraldehyde, and the ELVs were visualized with 1.4 nm of Nanogold and gold enhancement.

These studies showed that ELVs could interact with cilia in $<$1 min and that they were then cleared rapidly so that by 10 min few cilia had gold on their surface (Figure 7). The findings were consistent in IMCD cells (Figure 7) and BUs (Figure 8, A through F). At high magnifications, the gold staining appears in patches of 50 to 100 nm on the cilium (Figure 8, C and D, and G and H). Here, some of the gold patches are raised above the level of the shaft of the cilium, as though the interacting ELVs are adhering and perhaps fusing with the cilium. The rapid clearance of ELVs from the primary cilium, within approximately 10 min, suggests that they can integrate with the retrograde motors in the cilium[35] or detach or are degraded.

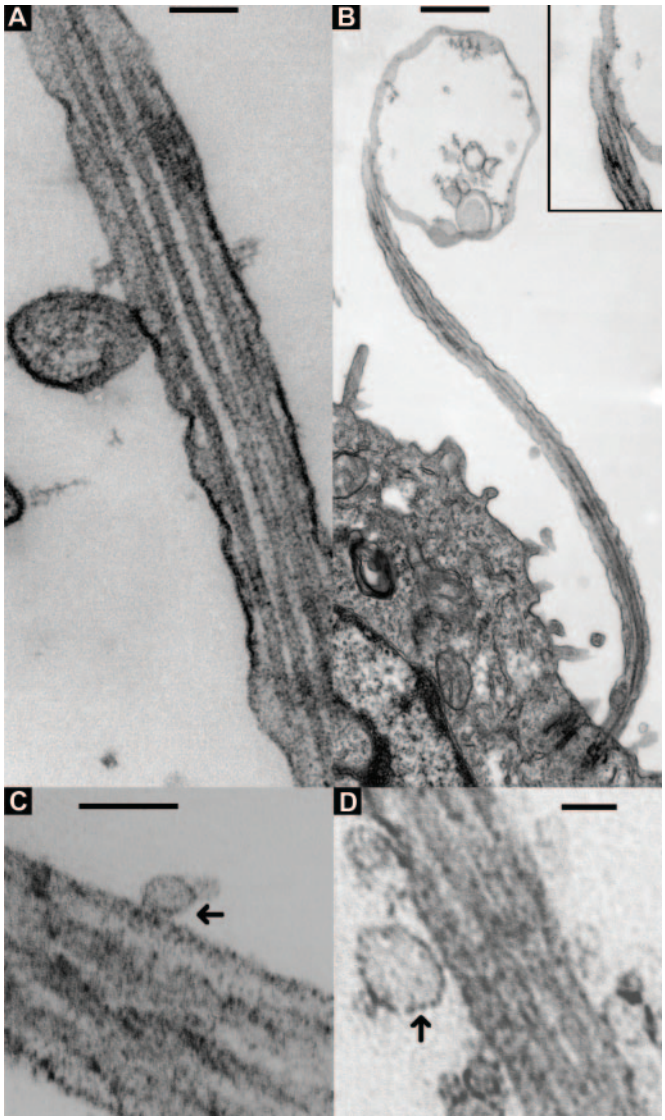

Figure 5. *In vivo* analysis of ELV–ciliary interactions in human ARPKD and the *Pkhd1*$^{del2/del2}$ mouse. (A and B) Transmission electron microscopy of primary cilia from the collecting duct of a neonate with mutation-proven ARPKD. (A) 120 nm diameter ELV adhering to the shaft of a primary cilium (bar = 100 nm). (B) A large MVB (1 to 2 μm) interacting with a primary cilium (bar = 500 nm). (Insert) Enlarged view of the adhesion site. Note the presence of two membranes at the site of attachment in both A and B. (C) ELVs interacting with a WT mouse biliary primary cilium (bar = 100 nm). (D) Accumulating ELVs on a biliary cholangiocyte primary cilium of a *Pkhd1*$^{del2/del2}$ mouse (bar = 100 nm). Note (arrows) the interaction seems to be an adhesive rather than a budding event.

In the biliary epithelia, there seem to be two populations of cilia: one capable of interacting with ELVs and another that lacks this ability. These act as an internal control for specificity (Figure 8, E and F), where BUs have been treated with PKD-ELVs for 2 min. One cilium is heavily decorated with gold detected on back-scatter, and one is not labeled.

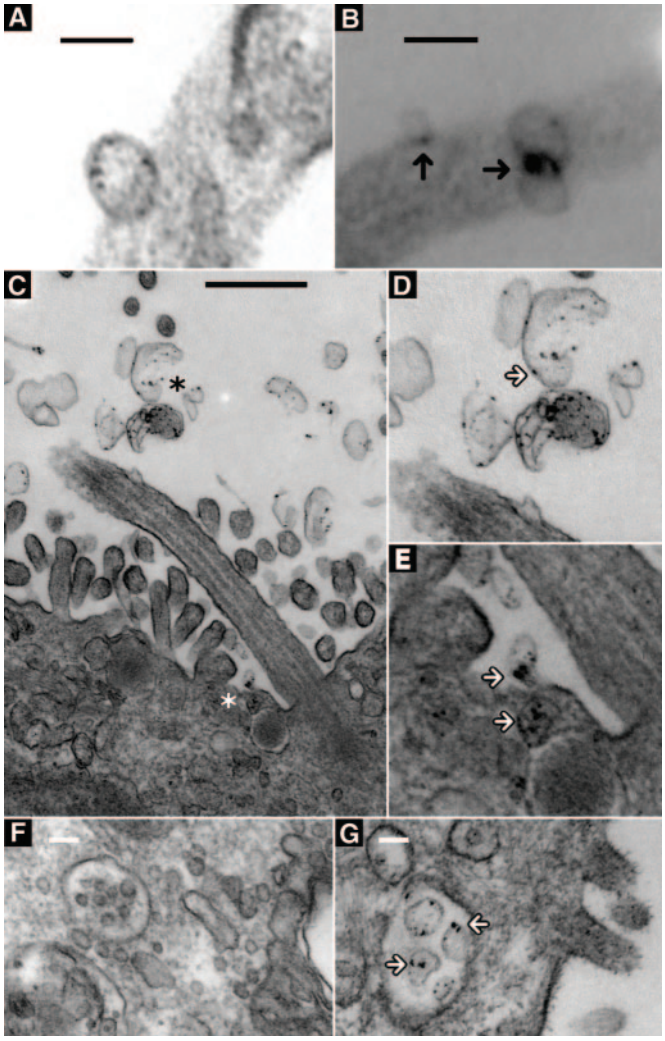

Figure 6. Location of PKD ELVs in wild-type rat biliary epithelium and *Pkhd1*$^{del2/del2}$ mouse biliary epithelium: (A and B) PC1 staining in *Pkhd1*$^{del2/del2}$ mouse biliary cilia using the PC1 monoclonal antibody 7e12 and nanogold with gold-on-gold enhancement. (A) An ELV adherent to the shaft of *Pkhd1*$^{del2/del2}$ mouse biliary primary cilium; no primary antibody, control (bar = 100 nm). (B) A cluster of PKD-ELVs interacting with a *Pkhd1*$^{del2/del2}$ mouse biliary primary cilium (black arrows) (bar = 100 nm). This shows that the vesicles/exosomes adherent to the primary cilium in the *Pkhd1*$^{del2/del2}$ mouse are PC1 positive. (C through G). TEM showing rat biliary epithelium stained with anti-PC1 as above; (C) wild-type rat biliary primary cilium stained with 7e12 showing apical membrane microvilli and a primary cilium shaft. Both are negative for PC1; however, the primary cilium is associated with nearby PC1 positive cup shaped ELVs (PKD-ELVs) (black asterisk) (scale bar = 500 nm). (D) An enlarged view of these (×2). (E) A PKD-ELV (white asterisk in C) extruding from an intracellular vesicle (perhaps an MVB) close to the base of the primary cilium (×3). (F and G) MVB origin of PC1+ ELVs. (F) Normal rat biliary epithelia showing an unstained MVB, no primary antibody (bar = 100 nm); (G) MVB showing ILVs (white arrows) positive for PC1 (bar = 100 nm). The bulk of PC1 staining is therefore restricted to the MVB and PKD-ELV.

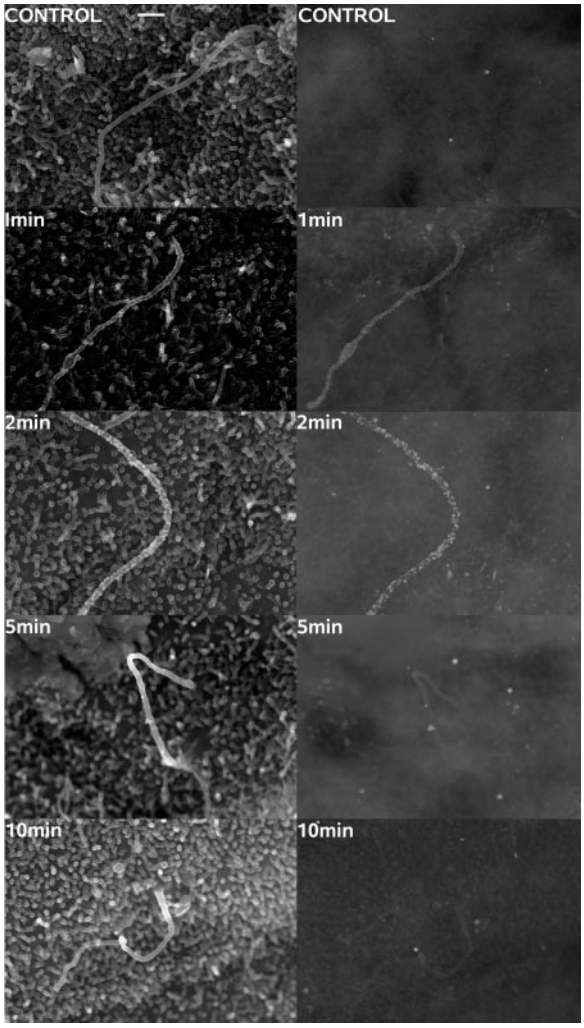

Figure 7. Biotinylated PKD-ELVs interact with primary cilia in IMCD3 cells. Biotinylated PKD-ELVs were applied to polarized IMCD3 cells for 1, 2, 5, and 10 min, then washed three times in Hanks' and fixed in 2.5% glutaraldehyde PBS. The ELVs were detected with 1.4 nm of Nanogold, enhanced using the autometallographic deposition of gold on gold, and then coated with carbon to a thickness of 15 nm. (Left) Standard SEMs of the IMCD (using secondary electrons). (Right) Images generated by backscattered electrons showing the distribution of gold and therefore exosomal protein. Control IMCDs were not treated with ELVs. Bar = 500 nm. Magnification, ×15,000.

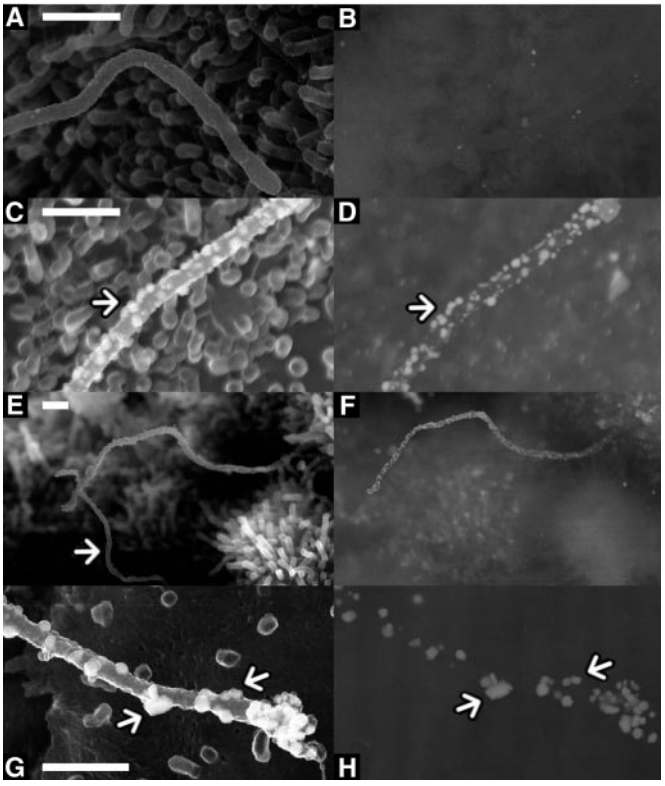

Figure 8. ELVs fuse with a subpopulation of primary cilia in BUs (primary biliary epithelial cells) and IMCD3 cells. (A, C, E, and G) secondary electrons; (B, D, F, and H) backscattered electrons. (A and B) Magnified view of a non–ELV-treated primary cilium. (C and D) Magnified view of a primary cilium treated with ELVs for 1 min. Note the raised areas on the cilium, suggesting that the ELVs are interacting with the cilium (examples arrowed). (E and F) Magnified primary cilia at 2 min, note that one cilium (arrowed) has no gold associated with it. (G and H) Magnified, SEM of an IMCD3 primary cilium treated with PKD-ELVs for 1 min. Note the raised blebs on the tip and shaft of this primary cilium (examples arrowed). Bars = 500 nm. Magnifications: ×60,000 in A through D; ×15,000 in E and F; ×80,000 in G and H.

DISCUSSION

Building on the work of Pisitkun *et al.*,[14] we developed new methods to resolve at least three different subpopulations of ELVs by density in human urine, enriched respectively for aquaporin 2, POD, and PC1/PC2/FCP/CD133 (the last group, we termed PKD-ELVs; Supplemental Figure 1). We characterized an extensive proteome from the PKD-ELVs and showed that both PC1 and FCP are cleaved *in vivo*. Finally, following up on our observations that mice with a targeted defect in the *Pkhd1* gene accumulate vesicles on primary cilia of cholangiocytes in dilated bile ducts, we showed that biotinylated PKD-ELVs can interact with the cilia of biliary and kidney epithelial cells.[19]

We characterized PKD-ELVs in detail and showed them to be abundant in PC1, PC2, and FCP by Western blot analysis, immunoelectron microscopy, and proteomics. PC1 and FCP are difficult to detect in normal adult kidneys, so the finding of a fraction where PC1, PC2, and FCP are abundant suggests functional relevance. The abundance of these proteins in the PKD-ELVs enabled us to ask questions about the *in vivo* processing of these proteins. We demonstrated that PC1 is highly glycosylated and that PC1 and FCP are cleaved *in vivo*, events that have previously been clearly visualized only in exogenous expression systems.[27–29] Analysis of the distribution of tryptic PC1 and FCP peptides with reference to the molecular weight of the parent protein (the molecular weight of the proteins in that particular gel slice) is consistent with PC1 cleavage at the GPS site and cleavage of FCP at the proprotein convertase site

(Supplemental Figures 2 and 3). Although these observations prove that cleavage occurs *in vivo*, they do not show exactly where the cleavage occurs.

PKD-ELVs contain many proteins found in exosomes from other sources, and our comparative analysis revealed considerable overlap with the proteome extracted from urinary exosomes by Pisitkun *et al.*[14]and with that isolated directly from urine[33]; however, we detected 232 proteins that were not present in these previous proteomes,[14,33] showing the unique nature of these vesicles (Figure 4, Supplemental Database 1a) and adding to the total urinary proteome identified to date. The PKD-ELV proteome is enriched in proteins involved in the biogenesis of ILVs, including all known members of the human ESCRT-III complex, and supports an MVB origin. This origin is further supported by the finding of PC1+ ILVs in rat cholangiocyte MVBs (Figure 6, F and G) and the presence of occasional multilaminate polycystin-positive structures in human urine (Figure 2I); however these ELVs contain only low levels of the exosomal marker CD63 and are rich in CD133. Initially, CD133 was thought to be an apical marker; however, recent studies confirmed that it also co-localizes with CD63 in intracellular vesicles.[36,37] Further characterization will be required to determine the origin of these vesicles that we have thus termed exosome-like vesicles.[36] Although much of our data support an MVB origin, budding from the apical membrane or even cilia cannot be ruled out.

Observations in the *Pkhd1*$^{del2/del2}$ mice showed that the primary cilia of the biliary tree are decorated with PC1+ structures that we assume are ELVs, and we therefore applied biotinylated ELVs to BU and IMCD3 cells. This resulted in the transfer of biotinylated protein to the primary cilia, whereas microvilli of the same cells showed minimal labeling. Furthermore, the interaction seemed specific because only a subpopulation of primary cilia could take up the label in BU (Figure 8, E and F). The ELV–cilium interaction probably depends on one or more ELV membrane proteins (the PKD-ELV proteome contains at least 96 of these). Adhesion candidate molecules are likely to be long: PC1 and FCP are predicted to have extracellular domains of at least 100 nm, approximately the size of an ELV. This size prediction is based on crystallography studies showing that the PKD1 domain is 4.4 nm long and is repeated 16 times in the extracellular region of PC1 (*i.e.*, total length approximately 70.4 nm).[38] There are also three other large domains in the extracellular portion of PC1: REJ (approximately 1000 amino acids), a C-type lectin (approximately 107 aa), and LRR domain (approximately 145 aa), yielding an overall length of approximately 100 nm.[4,5] These would significantly increase the functional adhesive area of ELVs (by approximately nine-fold). Because FCP contains multiple domains similar to those involved in host invasion (PA14 and PBH domains[8,39,40]), it is possible that this molecule behaves as an invasin and the accumulation of ELVs on the shaft of primary cilia in FCP (*PKHD1*) mutants may represent a failure of the invasion process, but FCP itself may not be responsible for the initial adhesion event.

Tanaka *et al.*[16] showed that, in the node, MVBs (termed NVPs) are released from the floor of the node and swept by nodal flow to the left side of the node, where they interact with the picket fence cilia. Symmetry breaking is associated with a PC2-dependent Ca^{2+} flux on the left side of the node.[17,18] We hypothesized that a similar process may be found in adult epithelia and that the rate of ELV interaction with cilia may be a proxy for flow.[11] Conversely, it is widely known that ciliary bending independent of exosomes causes an increase in intracellular calcium[41]; the exosome mechanism may not be a proxy for flow *per se* but acts as a separate and distinct flow-dependent mechanism. PKD-ELVs contain a wide range of signaling molecules: at least 48 GTPases and their associated proteins and four seven-membrane-spanning proteins (Smoothened, RAIG-1, RAIG-2, and RAIG-3; Table 2), with implications for cAMP signaling. cAMP has been shown to be a critical signaling molecule in both ADPKD and ARPKD, and therapies have been developed on the basis of lowering its level in the collecting duct and biliary epithelium.[42,43] Smoothened is present with its associated G_i proteins, but Hedgehog(s) or Patched(s) was not detectable in PKD-ELVs. If cilium–ELV interactions involve a fusion event, then we predict that active Smoothened will be delivered to the cilium with profound biologic consequences.[44]

In conclusion, PKD-ELVs and their interaction with primary cilia represent a new dimension to the biology of polycystic kidney and liver disease. This interaction unifies two disparate localizations for PC1 and raises the possibility of a novel form of "urocrine" and perhaps "bilocrine" signaling, fostering communication along the length of the nephron/biliary tree.

CONCISE METHODS

Isolation of Urinary ELVs

Urinary ELVs were isolated following a modification of the method of Zhou *et al.*[14,15] The first void of the day was collected, and one tablet of Complete proteinase inhibitor cocktail (Hoffmann-La Roche Inc., Nutley, New Jersey) was added. The urine was chilled and centrifuged at 15,000 × *g* for 15 min in an SLC-6000 rotor to remove cellular debris, filtered through an 8-μm nylon filter, and then centrifuged at

Table 2. Seven-transmembrane–spanning proteins found in PKD-ELVs

Access	Names	Rank	Unique Peptides	% Coverage
9NQ84	Retinoic acid-induced gene 3 protein (RAIG-3)	270	14	41
Q8NFJ5	Retinoic acid-induced protein 1 (RAIG-1)	440	8	23
Q9NZH0	Retinoic acid-induced gene 2 protein (RAIG-2)	482	7	18
Q99835	Smoothened homologue precursor (SMO) (Gx protein)	535	11	12

150,000 × *g* in a Sorvall T-647.5 rotor for 1 h. The pellet was resuspended in 1 ml of PBS 1× Complete at concentration of 2 mg/ml protein. This material was mainly composed of THP and some ELVs and was referred to as crude ELVs.

For removal of the THP from the preparation, 0.5 to 1.0 ml of crude ELVs were layered on top of a 5 to 30% sucrose gradient with D_2O as the solvent, buffered to pH 6.0 with 20 mM MES (the average pH of urine), generated using a BioComp Gradient Master Station (BioComp Instruments, Inc., Fredericton, NB, Canada). The gradient was centrifuged at 200,000 × *g* for 24 h in a Sorvall TH-641 rotor, and then the fractions were harvested by taking 14 fractions, 6-mm in length, from the 12-ml (Sorvall 06752) tube using a BioComp Gradient Master station. Fractions were diluted five- to 10-fold in PBS and centrifuged at 150,000 × *g* for 1 h in a Sorvall Surespin 630 rotor to recover PKD-ELVs. These were stored in 100 μl of 0.25 M Sucrose 20 mM HEPES (pH 7.4) with added Complete at −80°C.

Proteins were run on MOPS gels in normal water, stained and destained, and digested with trypsin again in normal water, diluting residual D_2O to background levels before proteomics and reversing any potential exchange reactions. The total time exposed to normal water was at least 5 d. The slowest proton exchange in denatured proteins is in the order of a few seconds at pH 7.0 at 20°C.[45] For this reason, the proteins were not accidentally labeled with deuterium because back-exchange was complete.

Use of Amino Reactive Biotinylation Reagents

For labeling ELVs with biotin, crude ELVs were dialyzed four times in a 10-kD cutoff dialysis cassette (Pierce, Rockford, IL) against 1 L of PBS (each dialysis was 20 min in duration). This removed free amines (urea) and small peptides. EZ-Link Sulfo-NHS-LC-Biotin [sulfosuccinimidyl-6-(biotinamido) hexanoate; Pierce] was added to a concentration of 2 mM to the ELVs and incubated on ice at 4°C for 30 min. The reaction was terminated by addition of glycine to a concentration of 20 mM. The ELVs were then loaded onto a 5 to 30% sucrose D_2O gradient. The efficacy of labeling was then assayed by running 0.1 μg of ELVs on a 4 to 12% SDS-PAGE gel and Western blotting with 1:10,000 streptavidin–horseradish peroxidase. This showed that the ELVs were biotinylated and the proteins were not degraded, the controls being negative (data not shown).

Isolation of Intrahepatic Bile Duct Segments, BUs

BUs were microdissected from normal rat liver using a proteinase-free modification of the protocol described by Roberts *et al.*[46] Briefly, rats were anesthetized with pentobarbital sodium (50 mg/kg intraperitoneally), then the portal vein was exposed and cannulated and the liver was perfused with ice-cold saline. Subsequently, 2 to 3 ml of liquid trypan blue agar was injected into the portal vein to facilitate identification of portal tracts. The liver was surgically removed and immersed in ice-cold preoxygenated HEPES-buffered saline (pH 7.4). After mechanical removal of the hepatic capsule and surface hepatocytes, intrahepatic bile ducts were exposed and microdissected using a Zeiss Stemi SV11 dissection microscope (Carl Zeiss MicroImaging, Inc., Thornwood, NY). The BUs were cut into 1.0- to 1.5-mm segments and transferred to a culture chamber. Viability was assessed by trypan blue exclusion; only BUs without evidence of trypan blue uptake were used. Viable BUs were then cut longitudinally and treated with ELVs at a protein concentration of 40 μg/ml in Hanks' buffered saline for 1 to 10 min, then washed twice in Hanks' and fixed in 2.5% glutaraldehyde for at least 1 h. BUs were then quenched in 100 mM glycine in PBS twice. Blocking of nonspecific sites was achieved with 0.5% BSA and 0.1% gelatin in PBS for 1 h. The BUs were then probed with a 1:100 dilution of 1.4 nm of Nanogold streptavidin for 30 min in the blocking reagent, then washed three times with PBS. Gold enhancement was done with a gold enhancement kit (Nanoprobes, Incorporated, Yaphank, NY). BUs were washed with water four to five times and dehydrated through ethanols 50-70-95-100-100-100%, each step for 3 to 5 min, then critical-point drying and carbon coating were performed. Carbon coating was for 15 to 20 nm thickness. Specimens were viewed with a Hitachi 4700 scanning electron microscope with secondary and backscattering beam (Hitachi America, Ltd., Brisbane, CA).

Participants

We obtained urine samples from normal human volunteers and a patient with ARPKD. Approval from the Mayo Institutional Review Board was obtained, and informed consent from each participant was given. Institutional Review Board approval and informed consent were obtained for the use of human tissue that would otherwise be considered surgical waste. Tissue was obtained for research after nephrectomy in a patient with ARPKD.

Mice and Rats

All procedures were conducted under protocols approved by the Institutional Animal Care and Use Committee at Mayo Clinic in accordance with the Animal Welfare Act and the Department of Health and Human Services.

ACKNOWLEDGMENTS

C.J.W. was funded by National Institutes of Health grant RO1 DK65056.

We thank Dr. Yiqiang Cai for the gift of Ab YCC2 to PC2, Dr. Thomas Hiesberger for the human FCP cDNA construct, Christopher J. Mason for the Bioinformatics searches, Jon E. Charlesworth for assistance with electron microscopy, and Dr. David H. Coombs for assistance with the Biocomp Gradient Master station.

DISCLOSURES

None.

REFERENCES

1. Torres V, Holley K, Offord K. Epidemiology. In: *Problems in Diagnosis and Management of Polycystic Kidney Disease*, edited by Grantham JJ, Kansas City: PKR Foundation Kansas City, 1985, pp 349–369
2. Wilson PD: Polycystic kidney disease. *N Engl J Med* 350: 151–164, 2004
3. The polycystic kidney disease 1 gene encodes a 14 kb transcript and lies within a duplicated region on chromosome 16. The European Polycystic Kidney Disease Consortium. *Cell* 77: 881–894, 1994
4. Polycystic kidney disease: The complete structure of the PKD1 gene

and its protein. The International Polycystic Kidney Disease Consortium. *Cell* 81: 289–298, 1995
5. Hughes J, Ward CJ, Peral B, Aspinwall R, Clark K, Millan JL, Gamble V, Harris PC: The polycystic kidney disease 1 (PKD1) gene encodes a novel protein with multiple cell recognition domains. *Nat Genet* 10: 151–160, 1995
6. Mochizuki T, Wu G, Hayashi T, Xenophontos SL, Veldhuisen B, Saris JJ, Reynolds DM, Cai Y, Gabow PA, Pierides A, Kimberling WJ, Breuning MH, Deltas CC, Peters DJ, Somlo S: PKD2, a gene for polycystic kidney disease that encodes an integral membrane protein. *Science* 272: 1339–1342, 1996
7. Ward CJ, Hogan MC, Rossetti S, Walker D, Sneddon T, Wang X, Kubly V, Cunningham JM, Bacallao R, Ishibashi M, Milliner DS, Torres VE, Harris PC: The gene mutated in autosomal recessive polycystic kidney disease encodes a large, receptor-like protein. *Nat Genet* 30: 259–269, 2002
8. Onuchic LF, Furu L, Nagasawa Y, Hou X, Eggermann T, Ren Z, Bergmann C, Senderek J, Esquivel E, Zeltner R, Rudnik-Schoneborn S, Mrug M, Sweeney W, Avner ED, Zerres K, Guay-Woodford LM, Somlo S, Germino GG: PKHD1, the polycystic kidney and hepatic disease 1 gene, encodes a novel large protein containing multiple immunoglobulin-like plexin-transcription-factor domains and parallel beta-helix 1 repeats. *Am J Hum Genet* 70: 1305–1317, 2002
9. Ward CJ, Yuan D, Masyuk TV, Wang X, Punyashthiti R, Whelan S, Bacallao R, Torra R, LaRusso NF, Torres VE, Harris PC: Cellular and subcellular localization of the ARPKD protein; fibrocystin is expressed on primary cilia. *Hum Mol Genet* 12: 2703–2710, 2003
10. Yoder BK, Hou X, Guay-Woodford LM: The polycystic kidney disease proteins, polycystin-1, polycystin-2, polaris, and cystin, are co-localized in renal cilia. *J Am Soc Nephrol* 13: 2508–2516, 2002
11. Nauli SM, Alenghat FJ, Luo Y, Williams E, Vassilev P, Li X, Elia AE, Lu W, Brown EM, Quinn SJ, Ingber DE, Zhou J: Polycystins 1 and 2 mediate mechanosensation in the primary cilium of kidney cells. *Nat Genet* 33: 129–137, 2003
12. Wang S, Zhang J, Nauli SM, Li X, Starremans PG, Luo Y, Roberts KA, Zhou J: Fibrocystin/polyductin, found in the same protein complex with polycystin-2, regulates calcium responses in kidney epithelia. *Mol Cell Biol* 27: 3241–3252, 2007
13. Wu Y, Dai X-Q, Li Q, Chen CX, Mai W, Hussain Z, Long W, Montalbetti N, Li G, Glynne R, Wang S, Cantiello HF, Wu G, Chen X-Z: Kinesin-2 mediates physical and functional interactions between polycystin-2 and fibrocystin. *Hum Mol Genet* 15: 3280–3292, 2006
14. Pisitkun T, Shen R-F, Knepper MA: Identification and proteomic profiling of exosomes in human urine. *Proc Natl Acad Sci U S A* 101: 13368–13373, 2004
15. Zhou H, Yuen PST, Pisitkun T, Gonzales PA, Yasuda H, Dear JW, Gross P, Knepper MA, Star RA: Collection, storage, preservation, and normalization of human urinary exosomes for biomarker discovery. *Kidney Int* 69: 1471–1476, 2006
16. Tanaka Y, Okada Y, Hirokawa N: FGF-induced vesicular release of Sonic hedgehog and retinoic acid in leftward nodal flow is critical for left-right determination. *Nature* 435: 172–177, 2005
17. Pennekamp P, Karcher C, Fischer A, Schweickert A, Skryabin B, Horst J, Blum M, Dworniczak B: The ion channel polycystin-2 is required for left-right axis determination in mice. *Curr Biol* 12: 938–943, 2002
18. McGrath J, Somlo S, Makova S, Tian X, Brueckner M: Two populations of node monocilia initiate left-right asymmetry in the mouse. *Cell* 114: 61–73, 2003
19. Woollard JR, Punyashtiti R, Richardson S, Masyuk TV, Whelan S, Huang BQ, Lager DJ, vanDeursen J, Torres VE, Gattone VH, LaRusso NF, Harris PC, Ward CJ: A mouse model of autosomal recessive polycystic kidney disease with biliary duct and proximal tubule dilatation. *Kidney Int* 72: 328–336, 2007
20. Ong AC, Harris PC, Davies DR, Pritchard L, Rossetti S, Biddolph S, Vaux DJ, Migone N, Ward CJ: Polycystin-1 expression in PKD1, early-onset PKD1, and TSC2/PKD1 cystic tissue. *Kidney Int* 56: 1324–1333, 1999
21. Cai Y, Maeda Y, Cedzich A, Torres VE, Wu G, Hayashi T, Mochizuki T, Park JH, Witzgall R, Somlo S: Identification and characterization of polycystin-2, the PKD2 gene product. *J Biol Chem* 274: 28557–28565, 1999
22. Lehtonen S, Ora A, Olkkonen VM, Geng L, Zerial M, Somlo S, Lehtonen E: *In vivo* interaction of the adapter protein CD2-associated protein with the type 2 polycystic kidney disease protein, polycystin-2. *J Biol Chem* 275: 32888–32893, 2000
23. Li Q, Montalbetti N, Shen PY, Dai X-Q, Cheeseman CI, Karpinski E, Wu G, Cantiello HF, Chen X-Z: Alpha-actinin associates with polycystin-2 and regulates its channel activity. *Hum Mol Genet* 14: 1587–1603, 2005
24. Zatti A, Chauvet V, Rajendran V, Kimura T, Pagel P, Caplan MJ: The C-terminal tail of the polycystin-1 protein interacts with the Na,K-ATPase alpha-subunit. *Mol Biol Cell* 16: 5087–5093, 2005
25. Parnell SC, Magenheimer BS, Maser RL, Rankin CA, Smine A, Okamoto T, Calvet JP: The polycystic kidney disease-1 protein, polycystin-1, binds and activates heterotrimeric G-proteins in vitro. *Biochem Biophys Res Commun* 251: 625–631, 1998
26. Parnell SC, Magenheimer BS, Maser RL, Zien CA, Frischauf A-M, Calvet JP: Polycystin-1 activation of c-Jun N-terminal kinase and AP-1 is mediated by heterotrimeric G proteins. *J Biol Chem* 277: 19566–19572, 2002
27. Kaimori J-Y, Nagasawa Y, Menezes LF, Garcia-Gonzalez MA, Deng J, Imai E, Onuchic LF, Guay-Woodford LM, Germino GG: Polyductin undergoes notch-like processing and regulated release from primary cilia. *Hum Mol Genet* 16: 942–956, 2007
28. Ponting CP, Hofmann K, Bork P: A latrophilin/CL-1-like GPS domain in polycystin-1. *Curr Biol* 9: R585–R588, 1999
29. Qian F, Boletta A, Bhunia AK, Xu H, Liu L, Ahrabi AK, Watnick TJ, Zhou F, Germino GG: Cleavage of polycystin-1 requires the receptor for egg jelly domain and is disrupted by human autosomal-dominant polycystic kidney disease 1-associated mutations. *Proc Natl Acad Sci U S A* 99: 16981–16986, 2002
30. Hou X, Mrug M, Yoder BK, Lefkowitz EJ, Kremmidiotis G, D'Eustachio P, Beier DR, Guay-Woodford LM: Cystin, a novel cilia-associated protein, is disrupted in the cpk mouse model of polycystic kidney disease. *J Clin Invest* 109: 533–540, 2002
31. Chiang AP, Nishimura D, Searby C, Elbedour K, Carmi R, Ferguson AL, Secrist J, Braun T, Casavant T, Stone EM, Sheffield VC: Comparative genomic analysis identifies an ADP-ribosylation factor-like gene as the cause of Bardet-Biedl syndrome (BBS3). *Am J Hum Genet* 75: 475–484, 2004
32. Fan Y, Esmail MA, Ansley SJ, Blacque OE, Boroevich K, Ross AJ, Moore SJ, Badano JL, May-Simera H, Compton DS, Green JS, Lewis RA, van Haelst MM, Parfrey PS, Baillie DL, Beales PL, Katsanis N, Davidson WS, Leroux MR: Mutations in a member of the Ras superfamily of small GTP-binding proteins causes Bardet-Biedl syndrome. *Nat Genet* 36: 989–993, 2004
33. Adachi J, Kumar C, Zhang Y, Olsen JV, Mann M: The human urinary proteome contains more than 1500 proteins, including a large proportion of membrane proteins. *Genome Biol* 7: R80, 2006
34. Sohara E, Luo Y, Zhang J, Manning DK, Beier DR, Zhou J: Nek8 regulates the expression and localization of polycystin-1 and polycystin-2. *J Am Soc Nephrol* 19: 469–476, 2008
35. Follit JA, Tuft RA, Fogarty KE, Pazour GJ: The intraflagellar transport protein IFT20 is associated with the Golgi complex and is required for cilia assembly. *Mol Biol Cell* 17: 3781–3792, 2006
36. Marzesco A-M, Janich P, Wilsch-Brauninger M, Dubreuil V, Langenfeld K, Corbeil D, Huttner WB: Release of extracellular membrane particles carrying the stem cell marker prominin-1 (CD133) from neural progenitors and other epithelial cells. *J Cell Sci* 118: 2849–2858, 2005
37. Fonseca AV, Bauer N, Corbeil D: The stem cell marker CD133 meets the endosomal compartment: New insights into the cell division of hematopoietic stem cells. *Blood Cells Mol Dis* 41: 194–195, 2008
38. Jing H, Takagi J, Liu J-h, Lindgren S, Zhang R-g, Joachimiak A, Wang

J-h, Springer TA: Archaeal surface layer proteins contain beta propeller PKD, and beta helix domains and are related to metazoan cell surface proteins. *Structure* 10: 1453–1464, 2002
39. Rigden DJ, Mello LV, Galperin MY: The PA14 domain, a conserved all-beta domain in bacterial toxins, enzymes, adhesins and signaling molecules. *Trends Biochem Sci* 29: 335–339, 2004
40. de Groot PW, Klis FM: The conserved PA14 domain of cell wall-associated fungal adhesins governs their glycan-binding specificity. *Mol Microbiol* 68: 535–537, 2008
41. Praetorius HA, Frokiaer J, Nielsen S, Spring KR: Bending the primary cilium opens Ca2+-sensitive intermediate-conductance K+ channels in MDCK cells. *J Membr Biol* 191: 193–200, 2003
42. Wang X, Ii VG, Harris PC, Torres VE: Effectiveness of vasopressin V2 receptor antagonists OPC-31260 and OPC-41061 on polycystic kidney disease development in the PCK rat. *J Am Soc Nephrol* 16: 846–851, 2005
43. Masyuk TV, Masyuk AI, Torres VE, Harris PC, Larusso NF: Octreotide inhibits hepatic cystogenesis in a rodent model of polycystic liver disease by reducing cholangiocyte adenosine 3′,5′-cyclic monophosphate. *Gastroenterology* 132: 1104–1116, 2007
44. Rohatgi R, Milenkovic L, Scott MP: Patched1 regulates hedgehog signaling at the primary cilium. *Science* 317: 372–376, 2007
45. Krishna MM, Hoang L, Lin Y, Englander SW: Hydrogen exchange methods to study protein folding. *Methods* 34: 51–64, 2004
46. Roberts SK, Kuntz SM, Gores GJ, LaRusso NF: Regulation of bicarbonate-dependent ductular bile secretion assessed by lumenal micropuncture of isolated rodent intrahepatic bile ducts. *Proc Natl Acad Sci U S A* 90: 9080–9084, 1993

Supplemental information for this article is available online at http://www.jasn.org/.